Electronic Supplementary Information

for

Solid solutions of flexible host−guest supramolecules for tuning molecular motion and phase transition

Xun-Hui Zhou, Ying Zeng, Shao-Bin Tang, Zi-Ru Yu, Li-Ming Cao, Zi-Yi Du* and Chun-Ting He

Experimental details

Materials and methods. All chemicals were obtained from commercial sources and used without further purification. FT-IR spectra were recorded on a Perkin-Elmer Spectrum One FT-IR spectrometer using KBr pellets from 4000 to 400 cm^{-1}. Powder X-ray diffraction (PXRD) patterns (Cu-Kα) were collected on a MiniFlex600 θ–2θ diffractometer. Thermogravimetric analysis (TGA) was carried out on a TA Q50 system at a heating rate of 10 K/min under a nitrogen atmosphere. Differential scanning calorimeter (DSC) measurement was performed on a TA Q2000 instrument at a heating/cooling rate of 10 K/min. The nuclear magnetic resonance (NMR) spectra were recorded on a Bruker Avance III 400 MHz spectrometer. The variable-temperature/frequency complex permittivities were measured under a vacuum environment, using a Tonghui TH2838 LCR meter at a heating rate of 1 K/min, and the polycrystalline samples were ground and pressed into tablets under a pressure of ca. 5 MPa.

Synthesis of 1. A mixture of CrO_3 (3 mmol), 18-crown-6 (3 mmol), $(C_2H_5NH_3)Br$ (3 mmol) and aqueous HBr (0.25 mmol/g; 3 g) was dissolved in acetonitrile. The resultant clear red solution was allowed to stand at room temperature. After two days later, red block-shaped crystals of **1** were deposited from the solution, in a ca. 75% yield based on Cr. The PXRD on bulky crystals indicated that the experimental pattern matches well with the simulated one (Fig. S10). IR data (KBr, cm^{-1}): 3439(m), 3155(m), 3110(s), 3021(m), 2996(m), 2910(s), 2824(m), 2595(m), 2522(m), 2361(m), 1963(m), 1611(m), 1536(m), 1472(m), 1351(s), 1251(m), 1101(vs), 947(vs), 900(m), 864(m), 831(s), 794(m), 528(m).

Synthesis of 2. The synthesis of **2** is similar to that of **1**, except that the $(C_2H_5NH_3)Br$ was replaced by $(BrC_2H_4NH_3)Br$. As a result, red column-shaped crystals of **2** were obtained in a ca. 80% yield based on Cr. The PXRD on bulky crystals indicated that the experimental pattern matches well with the simulated one (Fig. S10). IR data (KBr, cm^{-1}): 3444(m), 3146(m), 3084(m), 3027(m), 2902(s), 2827(m), 2621(m), 2361(m), 1966(m), 1596(m), 1527(m), 1473(m), 1433(m), 1351(s), 1284(m), 1250(m), 1104(vs), 947(vs), 899(m), 835(m), 573(m), 527(m).

Single-crystal X-ray crystallography. The single-crystal X-ray diffraction intensities for **1** and **2** at different temperatures were collected on a Rigaku XtaLAB P300DS single-crystal diffractometer equipped with graphite-monochromated Cu-Kα radiation (λ = 1.5418 Å), or a Smart ApexII CCD diffractometer equipped with a graphite-monochromated Mo-Kα radiation (λ = 0.71073 Å). Absorption corrections were applied by using multi-scan program REQAB or SADABS.[S1,S2] The structures were solved with direct methods and refined with a full-matrix least-squares technique with the *SHELXTL* program package.[S3] Anisotropic atomic displacement parameters were applied to all non-hydrogen atoms except the disordered 18-crown-6 molecule in **2β** phase, whereas all the hydrogen atoms were generated geometrically. Crystallographic data and structural refinements for **1** and **2** under different temperatures are summarized in Table S1. The geometries of hydrogen bonds in **1** and **2** at two different temperatures are listed in Tables S2 and S3, respectively. More details about the crystallographic data have been deposited as Supporting Information.

First-principles molecular dynamic (MD) simulation. The first-principles MD simulations of **1** at different

temperatures were performed with the Materials Studio 5.5 package,[S4] based on the density functional theory (DFT). Before the MD simulations, the geometries of all structures were optimized with the Dmol^3 module. The widely used generalized gradient approximation (GGA) with the Perdew-Burke-Ernzerhof (PBE) functional and the double numerical plus d-functions (DND) basis set were used for the non-metal atoms, while the effective core potentials (ECP) were employed for the metal atoms. Besides, thermal smearing for the orbital occupancy was used to accelerate convergence. Then, the simulations were performed in a constant-volume and constant-temperature (NVT) ensemble with the temperature set at 150 K for **1α**/**2α** and at 300 K for **1β**/**2β**. The simple Nosé-Hoover thermostat and random initial velocities method were used. The total simulation time was 6 ps for **1α** and 10 ps for **1β**/**2α**/**2β**, with a time step of 1.0 fs.

Table S1 Summary of crystal data and structural refinements for **1** and **2** at different phases

Empirical formula	$C_{14}H_{32}N_1O_9Br_1Cr_1$		$C_{14}H_{31}N_1O_9Br_2Cr_1$	
Formula weight	490.32		569.22	
Temperature (K)	150(2)	296(2)	150(2)	296(2)
Phase type	**1α**	**1β**	**2α**	**2β**
Space group	*Pna*2$_1$	*Pnma*	*P*−1	*P*−1
a (Å)	16.6558(3)	8.417(4)	8.7327(3)	8.6959(3)
b (Å)	11.3245(3)	11.396(5)	11.6396(4)	11.6717(5)
c (Å)	23.4109(4)	23.622(10)	12.0019(4)	12.2829(5)
α	90	90	107.718(2)	109.137(4)
β	90	90	100.411(2)	98.956(3)
γ	90	90	98.142(2)	98.155(3)
V/Å^3	4415.73(16)	2265.9(16)	1117.48(7)	1138.29(8)
Z	4	4	2	2
D_{calcd}/g cm^{-3}	1.475	1.437	1.692	1.661
μ/mm^{-1}	6.756	2.308	4.129	4.054
GOF on F^2	1.040	1.031	1.042	1.080
R_1, wR_2 [$I > 2\sigma(I)$][a]	0.0799, 0.2398	0.0569, 0.1587	0.0215, 0.0540	0.0571, 0.1444
R_1, wR_2 (all data)	0.0925, 0.2629	0.0872, 0.1825	0.0267, 0.0556	0.0828, 0.1592

[a] $R_1 = \sum||F_o| - |F_c||/\sum|F_o|$, $wR_2 = \{\sum w[(F_o)^2 - (F_c)^2]^2/\sum w[(F_o)^2]^2\}^{1/2}$

Table S2 The geometries (Å, °) of hydrogen bonds in **1** at two different temperatures

	D–H···A	D–H	H···A	D···A	D–H···A
150 K	N(1)–H(1C)···O(1)	0.890(7)	2.121(5)	2.904(8)	146.4(5)
	N(1)–H(1D)···O(5)	0.891(7)	2.056(7)	2.92(1)	163.2(5)
	N(1)–H(1E)···O(3)	0.890(7)	2.023(5)	2.865(8)	157.4(5)
	N(2)–H(2C)···O(12)	0.890(7)	2.084(5)	2.918(8)	155.5(5)
	N(2)–H(2D)···O(8)	0.890(7)	2.029(7)	2.92(1)	175.1(5)
	N(2)–H(2E)···O(10)	0.890(7)	1.995(6)	2.876(9)	170.5(5)
296 K	N(1)–H(1C)···O(2)	0.89(2)	1.927(2)	2.77(3)	156.6(5)
	N(1)–H(1D)···O(4)	0.889(7)	2.069(4)	2.934(6)	164.0(3)
	N(1)–H(1E)···O(2)#1	0.89(3)	2.187(2)	3.06(3)	166.4(7)

Symmetry codes: #1. *x*, 1/2 – *y*, *z*.

Table S3 The geometries (Å, °) of hydrogen bonds in **2** at two different temperatures

	D–H···A	D–H	H···A	D···A	D–H···A
150 K	N(1)–H(1C)···O(6)	0.88(2)	2.16(2)	2.938(2)	147(2)
	N(1)–H(1D)···O(2)	0.90(2)	2.03(2)	2.898(2)	161(2)
	N(1)–H(1E)···O(4)	0.89(2)	1.97(2)	2.858(2)	174(2)
296 K	N(1)–H(1C)···O(2)	0.895(3)	2.24(1)	2.98(1)	139.8(4)
	N(1)–H(1D)···O(2)	0.916(3)	2.01(1)	2.82(1)	147.3(4)
	N(1)–H(1E)···O(4)	0.881(4)	1.98(1)	2.85(1)	165.7(4)

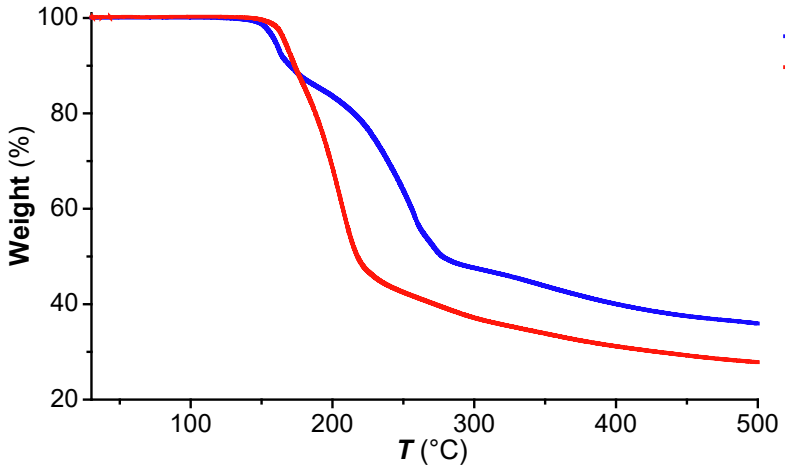

Fig. S1 TGA curves for **1** (red) and **2** (blue).

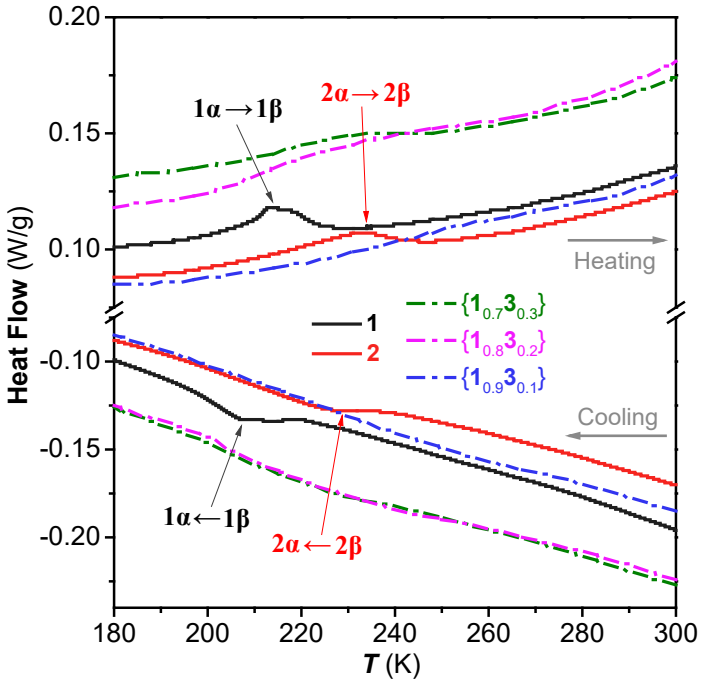

Fig. S2 DSC measurements for 1, 2 and their solid solutions, recorded on a heating–cooling cycle.

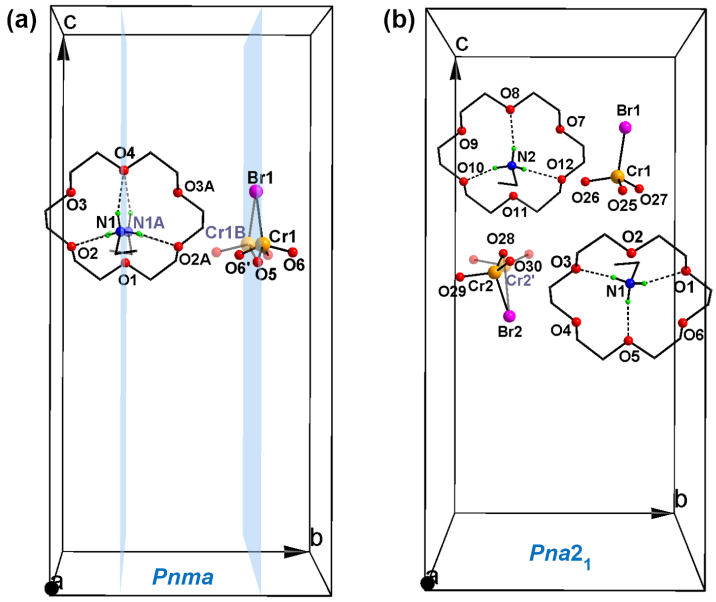

Fig. S3 Asymmetric units of **1β** (a) and **1α** (b). Symmetry code: A. *x*, 1/2 – *y*, *z*; B. *x*, 3/2 – *y*, *z*. The transparent blue planes in **1β** represent the mirror plane.

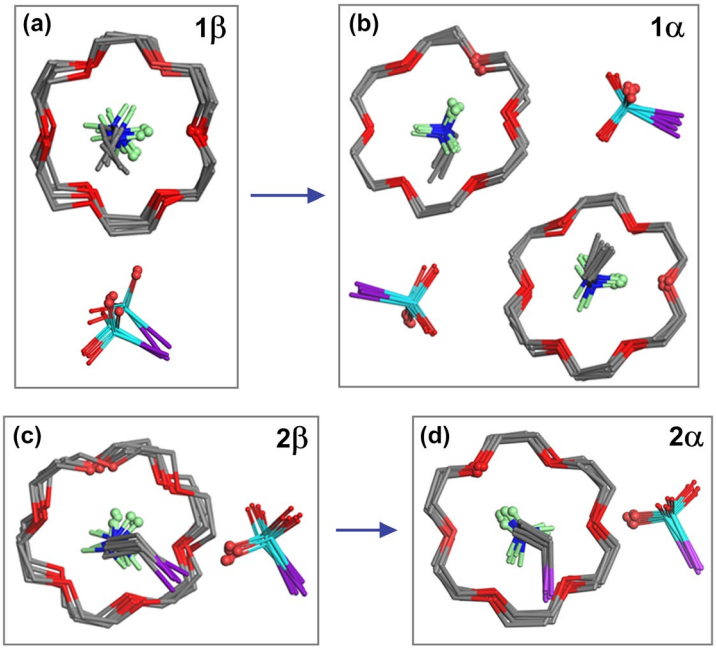

Fig. S4 Overlapping maps of the snapshots for the corresponding (18-crown-6)], $(C_2H_5NH_3)^+$/$(BrC_2H_4NH_3)^+$ and $[CrO_3Br]^-$ ions in **1β** (a), **1α** (b), **2β** (c) and **2α** (d), respectively, by NVT dynamic simulation over the simulation times of 1.0/2.0/3.0/4.0/5.0/6.0 ps in (b), and 2.5/4.0/5.5/7.0/8.5/10.0 ps in (a, c, d). The simulation temperature is 150 K for **1α**/**2α** and 300 K for **1β**/**2β**. The specific atoms are highlighted in ball to guide the eye.

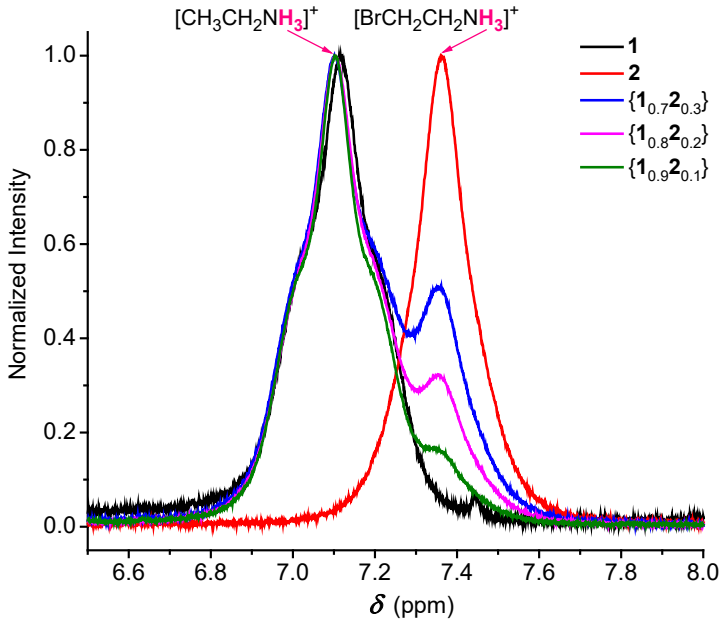

Fig. S5 The normalized ^{1}H NMR spectra of **1**, **2** and their solid solutions dissolved in deuterated acetonitrile, within the chemical shift range of 6.5 ~ 8.0 ppm.

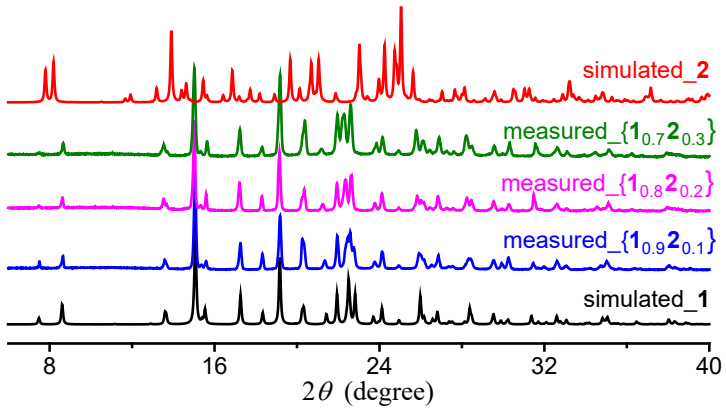

Fig. S6 Room-temperature PXRD patterns for the solid solutions {$\mathbf{1}_{1-x}\mathbf{2}_{x}$}. The mixing ratios ($x$) of **2** are 0.1, 0.2 and 0.3, resp ectively.

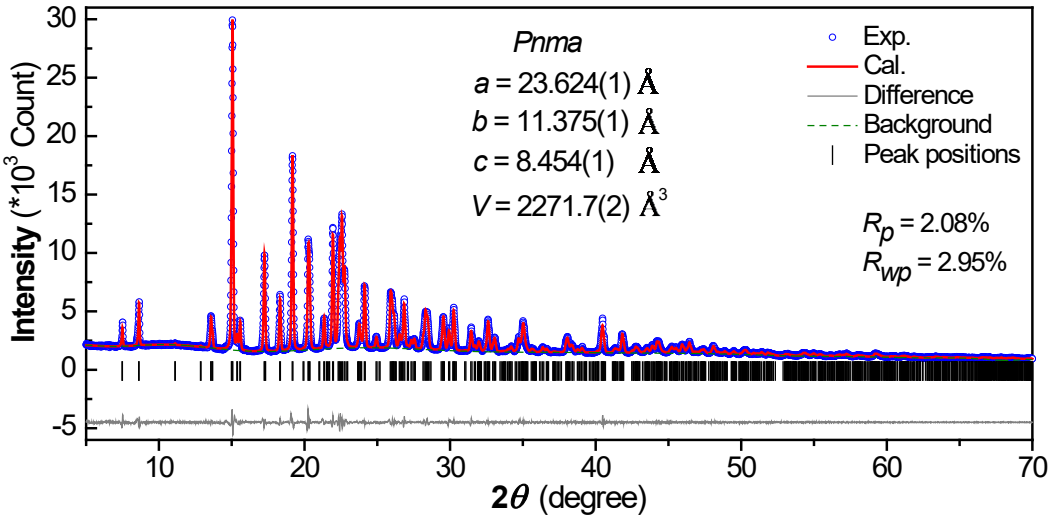

Fig. S7 Final Rietveld refinement result for solid solution {$\mathbf{1}_{0.9}\mathbf{2}_{0.1}$} at 296 K.

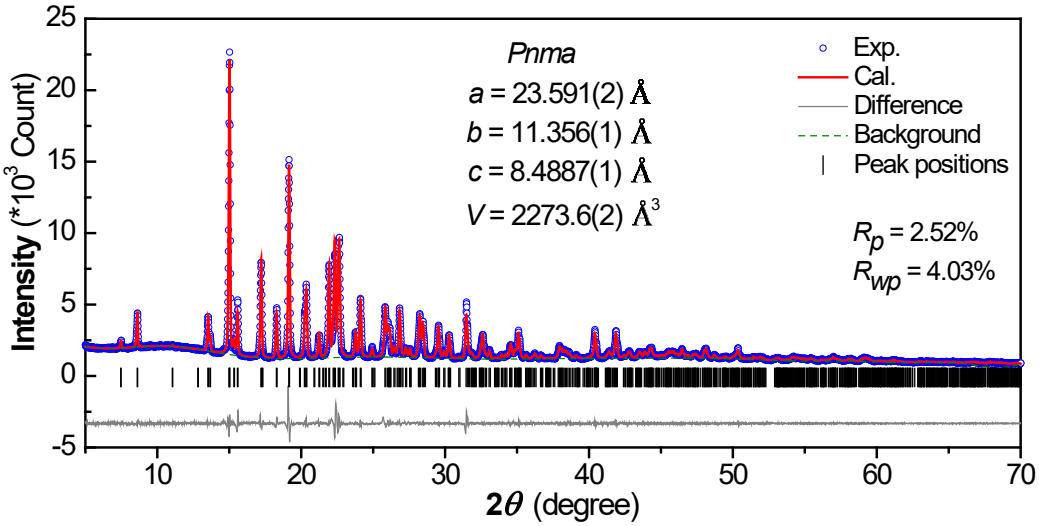

Fig. S8 Final Rietveld refinement result for solid solution {$\mathbf{1}_{0.8}\mathbf{2}_{0.2}$} at 296 K.

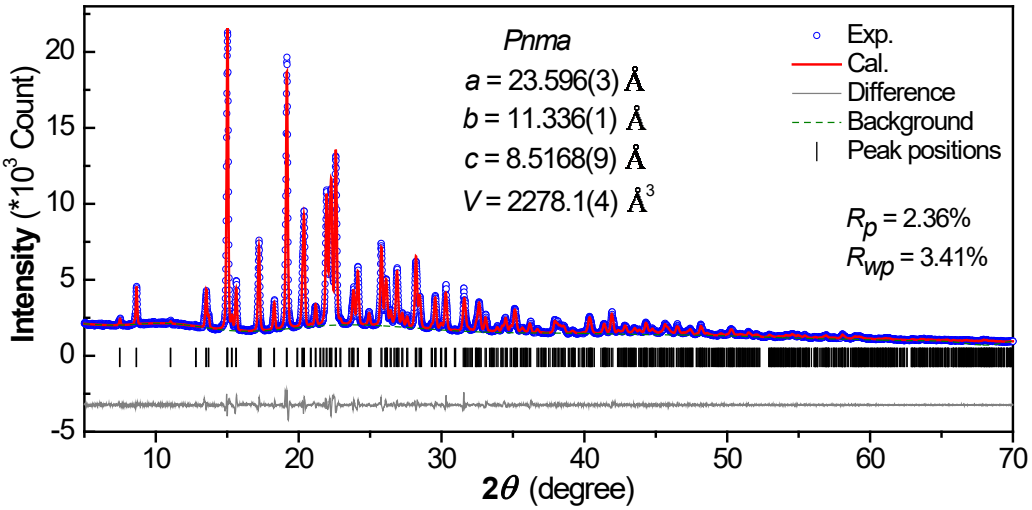

Fig. S9 Final Rietveld refinement result for solid solution {$\mathbf{1}_{0.7}\mathbf{2}_{0.3}$} at 296 K.

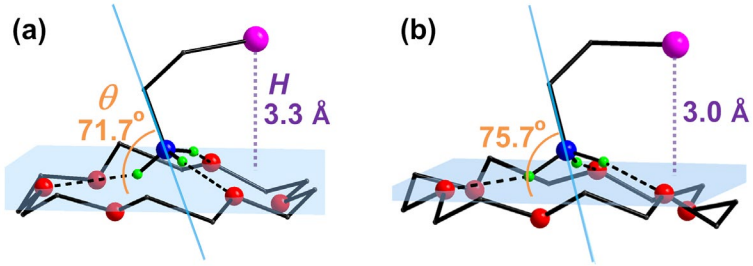

Fig. S10 Comparison of the geometries of the $[(BrC_2H_4NH_3)(18\text{-crown-}6)]^+$ group in **1β** (a) and the geometrically optimized model structure of solid solution {$\mathbf{1}_{0.75}\mathbf{2}_{0.25}$} (b).

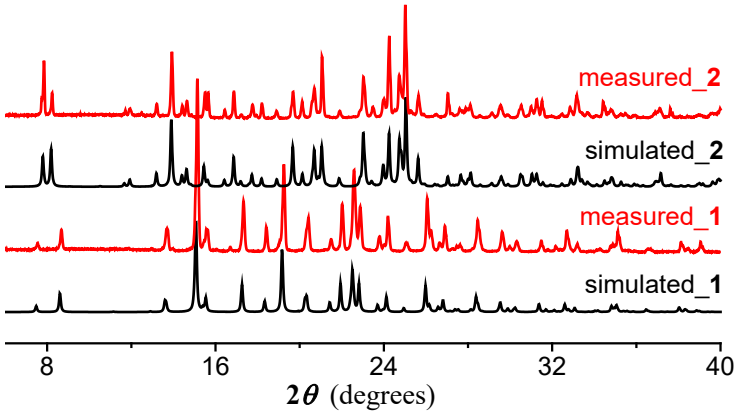

Fig. S11 Simulated and experimental PXRD patterns for **1** and **2** at room temperature.

References

S1 R. Jacobson, *REQAB*, Molecular Structure Corporation, The Woodlands, Texas, USA, **1998**.

S2 *APEX2*, *SADABS*, and *SAINT*; Bruker AXS Inc: Madison, Wisconsin, USA, **2008**.

S3 G. M. Sheldrick, *SHELX-96 program for crystal structure determination*, **1996**.

S4 Accelrys, Materials studio getting started, release 5.5; Accelrys Software, Inc.: San Diego, CA. **2009**.